HHS Public Access

Author manuscript

Exp Cell Res. Author manuscript; available in PMC 2016 April 10.

Published in final edited form as:

Exp Cell Res. 2015 April 10; 333(1): 39–48. doi:10.1016/j.yexcr.2015.02.002.

Phosphate Uptake-Independent Signaling Functions of the Type III Sodium-Dependent Phosphate Transporter, PiT-1, in Vascular Smooth Muscle Cells

Nicholas W. Chavkin[1], **Jia Jun Chia**[1], **Matthew H. Crouthamel**[1], and **Cecilia M. Giachelli**[1,*]

[1]Department of Bioengineering, University of Washington, Seattle, WA 98195, USA

Abstract

Vascular calcification (VC) is prevalent in chronic kidney disease and elevated serum inorganic phosphate (Pi) is a recognized risk factor. The type III sodium-dependent phosphate transporter, PiT-1, is required for elevated Pi-induced osteochondrogenic differentiation and matrix mineralization in vascular smooth muscle cells (VSMCs). However, the molecular mechanism(s) by which PiT-1 promotes these processes is unclear. In the present study, we confirmed that the Pi concentration required to induce osteochondrogenic differentiation and matrix mineralization of mouse VSMCs was well above that required for maximal Pi uptake, suggesting a signaling function of PiT-1 that was independent of Pi transport. Elevated Pi-induced signaling via ERK1/2 phosphorylation was abrogated in PiT-1 deficient VSMCs, but could be rescued by wild-type (WT) and a Pi transport-deficient PiT-1 mutant. Furthermore, both WT and transport-deficient PiT-1 mutants promoted osteochondrogenic differentiation as measured by decreased SM22α and increased osteopontin mRNA expression. Finally, compared to vector alone, expression of transport-deficient PiT-1 mutants promoted VSMC matrix mineralization, but not to the extent observed with PiT-1 WT. These data suggest that both Pi uptake-dependent and -independent functions of PiT-1 are important for VSMC processes mediating vascular calcification.

Keywords

PiT-1; SLC20A1; phosphate; calcification; ERK phosphorylation; signaling

Introduction

Vascular calcification (VC) is the inappropriate deposition of calcium phosphate salts in the vasculature and a strong predictor of cardiovascular morbidity and mortality [1]. Patients with chronic kidney disease-mineral bone disorder (CKD-MBD) have a greatly elevated risk for developing vascular calcification compared to the general population [2, 3], and

*Address Correspondence to: Cecilia M. Giachelli, Box 355061, Foege Hall, University of Washington, Seattle, WA 98195, Phone: 206-543-0205, Fax: 206-616-9763, ceci@uw.edu.

cardiovascular disease is the greatest risk for death in CKD-MBD patients [4]. Elevated serum phosphate (Pi) is a major driver of VC in CKD-MBD patients, and recognized as a non-traditional risk factor for cardiovascular mortality in these patients [5–7].

Elevated serum Pi has both indirect hormonal consequences as well direct procalcific effects on vascular cells that may contribute to VC and elevated cardiovascular risk. Hyperphosphatemia induces serum FGF-23 and PTH levels, thereby decreasing serum Pi by inhibiting type II Pi transporters in the proximal tubule of the kidneys and promoting renal Pi excretion [8]. Decreased 1,25-dihydroxyvitamin D helps normalize serum Pi by inhibiting type II Pi transporters in the intestine [9]. Elevated FGF23 and PTH, and deficient 1,25-dihydroxyvitamin D levels have all been associated with VC [10, 11], and may contribute to driving this pathology in CKD-MBD patients.

In addition to indirect effects, elevated Pi directly stimulates vascular smooth muscle cells (VSMCs) to undergo osteochondrogenic differentiation and matrix calcification ([12] for review). Knock-down of the type III sodium-dependent Pi transporter 1, PiT-1, greatly reduced matrix mineral deposition in human VSMC [13, 14], suggesting that PiT-1 was required for Pi-induced calcification. More recent studies have addressed the importance of PiT-1 in VSMC calcification in mice, and uncovered redundant roles with the related family member, PiT-2 [15]. Furthermore, PiT-1 has been shown to be required for elevated Pi-induced apoptosis in valve interstitial cells [16] and autophagy in VSMCs [14], both of which are important regulators of VC.

Although it is clear that elevated Pi directly induces VSMC calcification through PiT-1, the molecular mechanisms by which PiT-1 facilitates this process are still unclear. Furthermore, the concentration of Pi that induces matrix calcification (>2mM) in VSMCs is much higher than that required for maximal Pi uptake by PiT-1 in VSMCs (~0.5mM). This suggests that PiT-1 might have a signaling function independent of Pi uptake [13, 15, 17, 18]. To address this possibility, ERK1/2 phosphorylation, osteochondrogenic phenotype change, and matrix calcification were carefully examined in VSMC expressing wild-type and transport-deficient PiT-1 mutants. Our findings indicate that PiT-1 has both phosphate uptake-dependent and phosphate uptake-independent functions in VSMC related to VC.

Methods

Cell isolation and maintenance

Primary medial VSMCs were isolated from aortas of wild-type C57BL/6 (WT VSMC), PiT-1 flox/flox C57BL/6 (PiT-1 fl/fl VSMC), and PiT-1 flox/flox SM22αCre C57BL/6 (PiT-1 ΔSM VSMC) mice as previously described [15]. Briefly, aortas were removed from 4–5 week old mice, the medial layer was isolated and digested in collagen and elastin, and the primary (P0) VSMCs were incubated in T-25 flasks at 37° C and 5% CO_2 with Dulbecco's Modified Eagle Medium (DMEM, Life Technologies, 11995) supplemented with 20% Fetal Bovine Serum (FBS, HyClone), 1% antibiotic/antimycotic, 1% glutamine, and 1% non-essential amino acids (Life Technologies). VSMCs were passaged and maintained at 37° C and 5% CO_2 in normal growth media DMEM supplemented with 10% FBS and 1% antibiotic/antimycotic.

Pi uptake assay

Pi uptake was measured as previously described [19]. Briefly, VSMCs were seeded into 12-well tissue culture plates and incubated with radiolabeled $H_3{}^{33}PO_4$ (Perkin Elmer) and un-labeled potassium phosphate in either sodium-containing Earle's Balanced Salt Solution (EBSS) or sodium-free, choline-containing EBSS. VSMCs were incubated for 20 minutes, lysate was collected, and radioactive counts were recorded in OptiFluor (Perkin Elmer) using a LS 6500 Beckman liquid scintillation counter. Sodium-dependent Pi uptake was calculated by subtracting uptake in choline containing media from total uptake in sodium containing media, and normalized to incubation time and protein concentration of the cell lysate, quantified by Bicinchoninic Acid assay (Thermo Scientific). Michaelis-Menten kinetic parameters were determined by non-linear regression.

Calcification assay

Calcification was determined as previously described [19]. Briefly, VSMCs were grown in 6-well tissue culture plates in normal growth media until 70–80% confluent, then VSMCs were incubated with DMEM supplemented with 5% FBS, 1% antibiotic/antimycotic, and $Na_2PO_4/NaPO_4$ (pH = 7.4) to varying Pi concentrations. After 8 days, calcium was extracted with 0.6 N HCl at 4°C overnight. Calcium concentration was determined by the O-Cresolphthalein method using the Calcium Reagent Set (Teco Diagnostics). Protein lysate was collected in 0.2 N NaOH. Protein concentration was determined by Bicinchoninic Acid assay. Calcium data was normalized to protein data.

Real-time quantitative PCR

Collection of mRNA was performed with RNeasy Mini Kit (Qiagen) following manufacturer's protocol. Real-time quantitative PCR (Q-PCR) was performed with primers listed (Table 1). All Q-PCR gene counts were normalized to 18S gene counts and quantified using the quantitative ΔΔCt method.

Quantification of Pi-induced phosphorylated ERK1/2

VSMCs were grown in 6-well tissue culture plates in normal growth media. At 70–80% confluence, cells were washed twice with PBS and incubated in Pi-free DMEM (Life Technologies, 11971) supplemented with 1% FBS and 1% antibiotic/antimycotic. After 24 hours, media was aspirated and VSMCs were incubated in Pi-free DMEM supplemented with 1% FBS, 1% antibiotic/antimycotic, and $Na_2PO_4/NaPO_4$ (pH = 7.4) to varying Pi concentrations. After 5 or 15 minutes of incubation, VSMCs were washed three times with ice-cold PBS, and cell lysate was collected using lysate buffer (0.1 mM Tris pH 6.8 2% SDS) with added protease inhibitors and phosphatase inhibitors. Protein was loaded at 10ug/lane into 10% SDS-PAGE gels, transferred to PVDF membranes, and analyzed by immunoblot. Primary phosphorylated ERK1/2 and total ERK1/2 antibodies (Cell Signaling Technology) and secondary HRP-conjugated goat anti-rabbit antibody (Jackson ImmunoResearch) were used with Western Lighting (ECL) substrate to expose the protein signal. ImageJ software (NIH, Bethesda, MD) was used to quantify the densitometry of the bands.

Site-directed mutagenesis of mouse PiT-1 cDNA

A pLXIN vector containing wild-type mouse PiT-1 cDNA (PiT-1 WT), that was previously created [13], was used as the template for site-directed mutagenesis (QuikChange, Agilent Technologies). Primers were designed (QuikChange Primer Design Program, Agilent Technologies) to create Pi uptake deficient mutants (PiT-1-E74K, PiT-1-S132A, PiT-1-S623A) as shown in Table 1. Sequencing by the University of Washington Sequencing Center confirmed gene sequence.

Retroviral infection of primary mouse VSMCs

PiT-1 ΔSM VSMCs were transduced as previously described [13] with pLXIN vectors containing wild-type, Pi uptake-deficient PiT-1 mutants, or control (vector alone). Briefly, the pLXIN vectors were transfected into Ecotropic Phoenix Packaging Cell Lines (ATCC, SD 3444) with Lipofectamine 2000 (Life Technologies) to create retrovirus-conditioned media, which was used to infect PiT-1 ΔSM VSMCs. VSMCs were selected and maintained in 200 ug/mL G418 (Sigma).

Immunocytochemistry of PiT-1 ΔSM VSMCs expressing PiT-1 constructs

PiT-1 ΔSM VSMCs transduced as described above were grown in Nunc Lab-Tek Permanox 4-well chamber slides (Sigma) in growth media until 70–80% confluent. VSMCs were washed with PBS and fixed with 100% MeOH at −20°C for 20 minutes. Fixed cells were washed with PBS and probed for PiT-1 with a rabbit anti-mouse PiT-1 antibody primary (lab generated serum) and DyLight 549-Conjugated AffiniPure Donkey Anti-Rabbit IgG secondary (Jackson ImmunoResearch, final 1.5 μg/mL concentration). Cells were counterstained with DAPI at 1μg/mL for 5 minutes, mounted with ProLong Gold Antifade (Life Technologies), and imaged with a Nikon E800 Upright Microscope.

Apoptosis assay

Apoptosis was determined through FITC-conjugated Annexin V flow cytometry using the FITC Annexin V Apoptosis Detection Kit (BD Pharmagen), following manufacturer's protocol. Briefly, VSMCs were gently trypsinized with 0.05% trypsin in versene for 5 minutes, and the FITC-conjugated Annexin V antibody and Propidium iodide were used to stain the suspended VSMCs. VSMCs undergoing apoptosis was defined as Annexin V positive and PI negative.

Statistical analysis

SPSS software v16.0 (SPSS, Chicago, IL) was used to perform Student t-tests to compare means of two individual groups, and one-way ANOVA with post-hoc Tukey test to compare means of three or more individual groups. Linear regression to determine variable correlation and nonlinear regression to determine Michaelis-Menten parameters were performed using STATA version 12 (StataCorp). A p-value of less than 0.05 was considered statistically significant.

Results

Pi concentration dependence of Pi uptake, calcification, and osteochondrogenic phenotype change in mouse VSMCs

To determine the concentration-dependent effects of Pi on wild-type mouse aortic VSMCs, we examined sodium-dependent Pi uptake, calcification, and osteochondrogenic phenotype change over a range of Pi concentrations. Similar to previous findings [13, 15, 17], the rate of sodium dependent Pi uptake in wild-type VSMCs increased at Pi concentrations between 0.03 mM to 0.1 mM, and saturated at 0.5 mM, consistent with high-affinity low-capacity Pi transport (Figure 1A). In contrast, significant VSMC matrix mineralization was observed only at Pi concentrations at or above 2.4 mM (Figure 1B). Likewise OPN mRNA expression was significantly increased and SM22α mRNA expression was significantly decreased at a Pi concentration of 2.6 mM compared to 1.0 mM (Figures 1C and 1D). Importantly, PiT-1 mRNA levels were not significantly increased across the same range of Pi concentrations (data not shown), suggesting that an increase in the amount of PiT-1 made by VSMCs was not responsible for the Pi concentration dependence observed for VSMC calcification and osteochondrogenic phenotype change.

PiT-1 deficiency eliminates Pi-induced ERK1/2 phosphorylation in VSMCs

ERK1/2 phosphorylation was previously shown to be important for elevated Pi-induced osteochondrogenic differentiation of VSMCs [20]. To determine whether PiT-1 was required for ERK1/2 phosphorylation in VSMCs in response to elevated Pi, PiT-1 fl/fl VSMCs and PiT-1 ΔSM VSMCs were investigated. Elevated Pi induced ERK1/2 phosphorylation in PiT-1 fl/fl VSMCs in a dose- and time-dependent manner (Figure 2A). A 2-fold increase in ERK1/2 phosphorylation was observed in VSMCs treated with 3.0 mM for 15 min compared to 1.0 mM Pi treatment. Elevated sodium sulfate did not induce ERK1/2 phosphorylation in VSMCs, suggesting that this response was specific to elevated Pi and not a generalized response to increased anions. In contrast, Pi-induced ERK1/2 phosphorylation at 3.0 mM Pi was greatly diminished in VSMCs from PiT-1 ΔSM, and no induction between 3.0 mM and 1.0 mM Pi was observed (Figure 2). Finally, there was no difference between ERK1/2 phosphorylation in response to either 0.5 mM or 1.0 mM Pi in either cell line.

Generation and characterization of Pi uptake deficient PiT-1 mutants

Since Pi concentrations that induced matrix mineralization, osteochondrogenic differentiation, and ERK1/2 phosphorylation were well above the Km of Pi uptake by PiT-1, we considered that PiT-1 may be involved in cell signaling through a Pi uptake-independent pathway. To separate Pi uptake-dependent function from Pi uptake-independent function of PiT-1, transport deficient PiT-1 mutants were generated. Previous studies on human PiT-1 identified three amino acids critical to Pi uptake: E70, S128, S621 [21–23]. Point mutations of these amino acids inhibited Pi uptake through PiT-1 without affecting membrane localization [21–23]. Therefore, we generated the corresponding point mutations in mouse PiT-1: E74K, S132A, and S623A (Table 2).

PiT-1 WT, PiT-1 transport-defective mutants (PiT-1-E74K, PiT-1-S132A, and PiT-1-S623A), and vector alone were expressed in VSMCs lacking PiT-1(PiT-1 ΔSM VSMCs). Over-expression of these constructs in PiT-1 ΔSM VSMCs was confirmed by Q-PCR (Figure 3A). Immunofluorescent histochemistry established that PiT-1 WT and mutant constructs were appropriately localized to the plasma membrane of transduced VSMCs (Figure 3B). Since recent studies revealed an up-regulation of the related family member, PiT-2, when PiT-1 was deleted from osteoblast or smooth muscle cells *in vivo* [15, 24], PiT-2 RNA expression was examined in the engineered cell lines. PiT-1 overexpression in cultured primary VSMCs did not significantly alter PiT-2 mRNA expression levels (Figure 3C).

Reduced Pi uptake kinetics of PiT-1 ΔSM VSMCs overexpressing PiT-1 transport deficient mutants

Rate of sodium-dependent Pi uptake was measured across a range of Pi concentrations in PiT-1 ΔSM VSMCs expressing either vector control, PiT-1 WT, or the mutant constructs PiT-1-E74K, PiT-1-S132A, or PiT-1-S623A (Figure 4). As expected, overexpression of PiT-1 WT significantly increased the rate of sodium-dependent Pi uptake compared to vector control VSMCs at all Pi concentrations tested. The PiT-1-E74K mutant did not increase the rate of sodium-dependent Pi uptake compared to vector control, and VSMC containing this construct had the lowest Pi uptake rate of the three PiT-1 mutants. The PiT-1-S132A and PiT-1-S623A mutations had intermediate effects; Pi uptake rate was significantly less than VSMCs overexpressing PiT-1 WT at lower Pi concentrations, but similar to PiT-1 WT at higher Pi concentrations. These findings are consistent with calculated Pi uptake kinetic parameters of each cell line. Maximal velocity (Vmax) of Pi uptake into the VSMCs expressing PiT-1 WT, PiT-1-S132A, and PiT-1-S623A were 0.881, 0.736, 0.950 pmol Pi/ug/min, respectively, and were two- to three-fold higher than cells expressing vector control or PiT-1-E74K (0.408, 0.290 pmol Pi/ug/min, respectively). Furthermore, sodium-independent Pi uptake was not different between the cell lines containing the different PiT-1 mutants (data not shown). Subsequent experiments utilized the PiT-1-E74K mutant since it showed the least ability to transport Pi among the PiT-1 mutant constructs tested.

Pi-induced ERK1/2 phosphorylation mediated by PiT-1 is Pi uptake-independent

Since we found that PiT-1 was required for Pi-induced ERK1/2 phosphorylation in VSMCs, we investigated whether Pi transport by PiT-1 was required for this process. PiT-1 ΔSM VSMCs expressing vector control, PiT-1 WT, or PiT-1-E74K were treated with either normal (1.0 mM) or elevated (3.0 mM) Pi, and ERK1/2 phosphorylation was measured. As shown in Figure 5, VSMCs expressing PiT-1 WT and PiT-1-E74K, but not vector control, both showed an increase in ERK1/2 phosphorylation in response to elevated Pi treatment. Incubation in 3.0 mM Pi increased ERK1/2 phosphorylation by 34% in PiT-1 WT and 30% in PiT-1-E74K VSMCs compared to 1.0 mM Pi treatment. This result suggests that ERK1/2 signaling mediated by elevated Pi through PiT-1 was Pi uptake-independent.

Pi uptake-independent PiT-1 function promotes Pi-induced osteochondrogenic differentiation

In VSMCs, ERK1/2 phosphorylation is required for osteochondrogenic differentiation in response to elevated Pi [20]. To determine if Pi uptake-independent PiT-1 functions promote VSMC phenotype change via ERK1/2 phosphorylation, we examined RNA expression of the osteochondrogenic lineage marker, OPN, and smooth muscle lineage marker, SM22α, in VSMCs expressing vector control, PiT-1 WT, or PiT-1-E74K. Expression of either PiT-1 WT or PiT-1-E74K greatly reduced SM22α mRNA levels compared to vector control (Figure 6A). This effect was observed even under normal Pi conditions, suggesting that increased PiT-1 expression, independent of extracellular Pi levels, promotes down-regulation of SM22α. Furthermore, as shown in Figure 6, OPN was induced to a greater extent in VSMCs expressing PiT-1 WT and PiT-1-E74K compared to vector control (Figure 6B). Down-regulation of SM22α and up-regulation of OPN is consistent with increased VSMC osteochondrogenic differentiation in VSMCs expressing PiT-1 WT or PiT-1-E74K.

PiT-1 promotes VSMC matrix mineralization via Pi uptake-dependent and Pi uptake-independent processes

PiT-1 expression has previously been shown to be required for elevated Pi-induced VSMC matrix mineralization [13], but whether Pi uptake through PiT-1 was required for this activity has not been determined. To address this, VSMCs expressing vector control, PiT-1 WT, or PiT-1-E74K were induced to mineralize with elevated Pi. Elevated Pi (2.6 mM) promoted calcification of all three VSMC lines compared to normal Pi conditions (1.0 mM). To rule out potential effects of PiT-1 on cell death in response to elevated Pi, apoptosis rates in vector control, PiT-1 WT, and PiT-1-E74K expressing VSMCs in normal and elevated Pi conditions were measured. Rates of apoptosis were less than 5% in all conditions tested, and elevated Pi did not induce apoptosis compared to normal Pi conditions (Figure 7B).

While VSMCs expressing PiT-1 WT showed the greatest induction, PiT-1-E74K expressing VSMCs also showed significantly greater mineralization than vector control VSMCs (Figure 7A). Furthermore, VSMCs expressing PiT-1-S132A and PiT-1-S623A (mutants with intermediate phosphate uptake properties) mineralized more than VSMC expressing PiT-1-E74K (Figure 7B). Though statistically significant, matrix mineralization in VSMCs was poorly correlated with calculated Vmax values of VSMC Pi uptake ($R^2 = 0.25$), suggesting that PiT-1 functions besides phosphate uptake contribute to maximal VSMC matrix mineralization.

Discussion

The present study addressed the hypothesis that PiT-1 mediates both phosphate uptake-dependent and -independent functions important for Pi-induced calcification in VSMC. PiT-1 deficient VSMC showed attenuated ERK1/2 phosphorylation compared to controls in response to elevated Pi. Transduction with both WT and transport deficient PiT-1 mutants restored Pi-inducible ERK1/2 phosphorylation in PiT-1 deficient VSMC. Moreover, VSMC osteochondrogenic differentiation was similar in VSMC expressing WT and transport deficient PiT-1 mutants. Finally, Pi transport-deficient mutants enhanced VSMC

calcification, though at lower levels than PiT-1 WT. These data suggest that PiT-1 signaling through ERK1/2 and downstream regulation of osteochondrogenic gene expression occurs via a Pi uptake-independent pathway, and that both Pi uptake-dependent and -independent processes play a role in promoting Pi-induced calcification.

The importance of ERK1/2 phosphorylation in osteochondrogenic differentiation and matrix mineralization of VSMCs in response to elevated Pi has been previously established [20, 25, 26]. In the present study, we extended these findings by determining that PiT-1 was required for Pi-induced ERK1/2 phosphorylation in VSMC. These results are consistent with findings in chondrocytes and HEK293 cells that showed decreased Pi-induced ERK1/2 phosphorylation following PiT-1 knock-down by siRNA [25, 26]. Furthermore, our studies are the first to show that PiT-1 induction of ERK1/2 phosphorylation in VSMC in response to elevated Pi can occur in the absence of Pi uptake through PiT-1.

In addition to ERK1/2 phosphorylation, Pi-induced regulation of genes downstream of ERK1/2 signaling, including SM22α and OPN, was supported by both WT and transport-defective PiT-1. Additionally, we observed that overexpression of either PiT-1-WT or PiT-1-E74K caused down-regulation of SM22α in normal Pi conditions, suggesting that the PiT-1 signaling pathway might be active under normal Pi conditions when PiT-1 density is very high. Our findings of a signaling function for PiT-1 are consistent with growing evidence in several other cell types for transport-independent functions of PiT-1. Beck et al. showed that PiT-1 silencing reduced cell proliferation, and that overexpression of a Pi uptake-deficient PiT-1 mutant could rescue this process in HeLa cells [22]. Also, Salaun et al. showed that a Pi uptake-deficient PiT-1 mutant reduced the rate of apoptosis in HeLa cells treated with Tumor Necrosis Factor-α [23]. Finally, PiT-1 regulation of hematopoietic stem cell differentiation was found to be Pi uptake-independent [27, 28]. However, none of those studies identified the cell signaling pathway required for transport-independent PiT-1 functions. Our findings suggest that ERK1/2 cell signaling is required for the PiT-1 response to elevated Pi, and further studies are warranted to investigate potential adaptor proteins that are responsible for PiT-1 signaling through ERK1/2. Since ERK kinases have been implicated in control of proliferation, apoptosis, and differentiation [29–31], it is interesting to speculate that the PiT-1 driven ERK1/2 signaling pathway that we have identified here might be involved in these processes as well.

Although transport defective PiT-1 was able to support elevated Pi-induced ERK1/2 phosphorylation and osteochondrogenic differentiation at levels similar to WT PiT-1, this was not the case for VSMC matrix mineralization. Both Pi uptake-dependent and Pi uptake-independent functions of PiT-1 were required to promote maximal VSMC matrix mineralization. These findings suggest that Pi uptake-dependent and -independent mechanisms regulate distinct cellular functions in VSMCs that work in concert to promote matrix mineralization depending on the level of extracellular Pi. One possibility is that at normal ambient Pi of 1.0 mM, the Pi transport function of PiT-1 predominates, and allows Pi entry into VSMC for essential cell functions with excess Pi shed from the cell via efflux transporters or matrix vesicles [32–34]. In contrast, at high ambient Pi (>2.0 mM), PiT-1 activates ERK1/2 and drives osteochondrogenic phenotype change, thereby promoting the loading of matrix vesicles not only with Pi, but also with pro-calcific cargo making them

"calcification competent". The importance of Pi-loaded matrix vesicles in initiating VSMC mineralization has been extensively studied, and osteochondrogenic differentiation of VSMC has been shown to enhance formation of calcification competent matrix vesicles by loading them with pro-calcific molecules such as alkaline phosphatase, and removing calcium mineral inhibitors including matrix GLA protein and Fetuin-A [33, 34]. Clearly, further investigations are required to test these exciting possibilities, and to determine the molecular mechanism by which PiT-1 senses extracellular Pi levels.

In conclusion, our findings suggest that at extracellular Pi concentrations above physiological levels, PiT-1 acts as a phosphate sensor with cell signaling functions that regulate E11K kinase activity, VSMC osteochondrogenic differentiation, and calcification. This possibility would help explain the strikingly different Pi-dependence of phosphate uptake (maximal 0.5 mM) versus VSMC differentiation and calcification (occurring above 2.0 mM). Further studies to delineate the mechanisms by which PiT-1 acts as a Pi sensor are warranted, and will help identify new therapeutic targets for treatment of VC.

Acknowledgements

This study received funding by the National Institutes of Health grant to Dr. Giachelli (1101 HL062329). N.W. Chavkin received funding from T32 EB001650 (NIBIB). M.H. Crouthamel received funding from T32 HL007828 (NHLBI). J. Chia received funding by a grant to the University of Washington from the Howard Hughes Medical Institute. The content of this study is solely the responsibility of the authors and does not necessarily represent the official views of the National Institutes of Health or other acknowledged funding sources.

References

1. Detrano R, Guerci AD, Carr JJ, Bild DE, Burke G, Folsom AR, Liu K, Shea S, Szklo M, Bluemke DA, O'Leary DH, Tracy R, Watson K, Wong ND, Kronmal RA. Coronary calcium as a predictor of coronary events in four racial or ethnic groups. N Engl J Med. 2008; 358:1336–1345. [PubMed: 18367736]
2. Shroff RC, McNair R, Figg N, Skepper JN, Schurgers L, Gupta A, Hiorns M, Donald AE, Deanfield J, Rees L, Shanahan CM. Dialysis accelerates medial vascular calcification in part by triggering smooth muscle cell apoptosis. Circulation. 2008; 118:1748–1757. [PubMed: 18838561]
3. Nakamura S, Ishibashi-Ueda H, Niizuma S, Yoshihara F, Horio T, Kawano Y. Coronary calcification in patients with chronic kidney disease and coronary artery disease. Clin J Am Soc Nephrol. 2009; 4:1892–1900. [PubMed: 19833908]
4. Tonelli M, Wiebe N, Culleton B, House A, Rabbat C, Fok M, McAlister F, Garg AX. Chronic kidney disease and mortality risk: a systematic review. J Am Soc Nephrol. 2006; 17:2034–2047. [PubMed: 16738019]
5. Block GA, Hulbert-Shearon TE, Levin NW, Port FK. Association of serum phosphorus and calcium × phosphate product with mortality risk in chronic hemodialysis patients: a national study. Am J Kidney Dis. 1998; 31:607–617. [PubMed: 9531176]
6. Young EW, Albert JM, Satayathum S, Goodkin DA, Pisoni RL, Akiba T, Akizawa T, Kurokawa K, Bommer J, Piera L, Port FK. Predictors and consequences of altered mineral metabolism: the Dialysis Outcomes and Practice Patterns Study. Kidney Int. 2005; 67:1179–1187. [PubMed: 15698460]
7. Adeney KL, Siscovick DS, Ix JH, Seliger SL, Shlipak MG, Jenny NS, Kestenbaum BR. Association of serum phosphate with vascular and valvular calcification in moderate CKD. J Am Soc Nephrol. 2009; 20:381–387. [PubMed: 19073826]
8. Hruska KA, Mathew S, Lund R, Qiu P, Pratt R. Hyperphosphatemia of chronic kidney disease. Kidney Int. 2008; 74:148–157. [PubMed: 18449174]

9. Kestenbaum B. Phosphate metabolism in the setting of chronic kidney disease: significance and recommendations for treatment. Semin Dial. 2007; 20:286–294. [PubMed: 17635817]
10. Levin A, Bakris GL, Molitch M, Smulders M, Tian J, Williams LA, Andress DL. Prevalence of abnormal serum vitamin D, PTH, calcium, and phosphorus in patients with chronic kidney disease: results of the study to evaluate early kidney disease. Kidney Int. 2007; 71:31–38. [PubMed: 17091124]
11. Isakova T, Wahl P, Vargas GS, Gutiérrez OM, Scialla J, Xie H, Appleby D, Nessel L, Bellovich K, Chen J, Hamm L, Gadegbeku C, Horwitz E, Townsend RR, Anderson CA, Lash JP, Hsu CY, Leonard MB, Wolf M. Fibroblast growth factor 23 is elevated before parathyroid hormone and phosphate in chronic kidney disease. Kidney Int. 2011; 79:1370–1378. [PubMed: 21389978]
12. Shanahan CM, Crouthamel MH, Kapustin A, Giachelli CM. Arterial calcification in chronic kidney disease: key roles for calcium and phosphate. Circ Res. 2011; 109:697–711. [PubMed: 21885837]
13. Li X, Yang HY, Giachelli CM. Role of the sodium-dependent phosphate cotransporter, Pit-1, in vascular smooth muscle cell calcification. Circ Res. 2006; 98:905–912. [PubMed: 16527991]
14. Dai XY, Zhao MM, Cai Y, Guan QC, Zhao Y, Guan Y, Kong W, Zhu WG, Xu MJ, Wang X. Phosphate-induced autophagy counteracts vascular calcification by reducing matrix vesicle release. Kidney Int. 2013; 83:1042–1051. [PubMed: 23364520]
15. Crouthamel MH, Lau WL, Leaf EM, Chavkin NW, Wallingford MC, Peterson DF, Li X, Liu Y, Chin MT, Levi M, Giachelli CM. Sodium-dependent phosphate cotransporters and phosphate-induced calcification of vascular smooth muscle cells: redundant roles for PiT-1 and PiT-2. Arteriosclerosis, thrombosis, and vascular biology. 2013; 33:2625–2632.
16. El Husseini D, Boulanger MC, Fournier D, Mahmut A, Bossé Y, Pibarot P, Mathieu P. High expression of the Pi-transporter SLC20A1/Pit1 in calcific aortic valve disease promotes mineralization through regulation of Akt-1. PLoS One. 2013; 8:e53393. [PubMed: 23308213]
17. Villa-Bellosta R, Bogaert YE, Levi M, Sorribas V. Characterization of phosphate transport in rat vascular smooth muscle cells: implications for vascular calcification. Arteriosclerosis, thrombosis, and vascular biology. 2007; 27:1030–1036.
18. Ravera S, Virkki LV, Murer H, Forster IC. Deciphering PiT transport kinetics and substrate specificity using electrophysiology and flux measurements. Am J Physiol Cell Physiol. 2007; 293:C606–C620. [PubMed: 17494632]
19. Jono S, McKee MD, Murry CE, Shioi A, Nishizawa Y, Mori K, Morii H, Giachelli CM. Phosphate regulation of vascular smooth muscle cell calcification. Circ Res. 2000; 87:E10–E17. [PubMed: 11009570]
20. Speer MY, Yang HY, Brabb T, Leaf E, Look A, Lin WL, Frutkin A, Dichek D, Giachelli CM. Smooth muscle cells give rise to osteochondrogenic precursors and chondrocytes in calcifying arteries. Circ Res. 2009; 104:733–741. [PubMed: 19197075]
21. Bøttger P, Pedersen L. Mapping of the minimal inorganic phosphate transporting unit of human PiT2 suggests a structure universal to PiT-related proteins from all kingdoms of life. BMC Biochem. 2011; 12:21. [PubMed: 21586110]
22. Beck L, Leroy C, Salaün C, Margall-Ducos G, Desdouets C, Friedlander G. Identification of a novel function of PiT1 critical for cell proliferation and independent of its phosphate transport activity. J Biol Chem. 2009; 284:31363–31374. [PubMed: 19726692]
23. Salaün C, Leroy C, Rousseau A, Boitez V, Beck L, Friedlander G. Identification of a novel transport-independent function of PiT1/SLC20A1 in the regulation of TNF-induced apoptosis. J Biol Chem. 2010; 285:34408–34418. [PubMed: 20817733]
24. Bourgine A, Pilet P, Diouani S, Sourice S, Lesoeur J, Beck-Cormier S, Khoshniat S, Weiss P, Friedlander G, Guicheux J, Beck L. Mice with hypomorphic expression of the sodium-phosphate cotransporter PiT1/Slc20a1 have an unexpected normal bone mineralization. PLoS One. 2013; 8:e65979. [PubMed: 23785462]
25. Kimata M, Michigami T, Tachikawa K, Okada T, Koshimizu T, Yamazaki M, Kogo M, Ozono K. Signaling of extracellular inorganic phosphate up-regulates cyclin D1 expression in proliferating chondrocytes via the Na+/Pi cotransporter Pit-1 and Raf/MEK/ERK pathway. Bone. 2010; 47:938–947. [PubMed: 20709201]

26. Yamazaki M, Ozono K, Okada T, Tachikawa K, Kondou H, Ohata Y, Michigami T. Both FGF23 and extracellular phosphate activate Raf/MEK/ERK pathway via FGF receptors in HEK293 cells. J Cell Biochem. 2010; 111:1210–1221. [PubMed: 20717920]

27. Liu L, Sánchez-Bonilla M, Crouthamel M, Giachelli C, Keel S. Mice lacking the sodium-dependent phosphate import protein, PiT1(SLC20A1), have a severe defect in terminal erythroid differentiation and early B cell development. Exp Hematol. 2013; 41:432.e7–443.e7. [PubMed: 23376999]

28. Beck L, Leroy C, Beck-Cormier S, Forand A, Salaün C, Paris N, Bernier A, Ureña-Torres P, Prié D, Ollero M, Coulombel L, Friedlander G. The phosphate transporter PiT1 (Slc20a1) revealed as a new essential gene for mouse liver development. PLoS One. 2010; 5:e9148. [PubMed: 20161774]

29. Meloche S, Pouysségur J. The ERK1/2 mitogen-activated protein kinase pathway as a master regulator of the G1- to S-phase transition. Oncogene. 2007; 26:3227–3239. [PubMed: 17496918]

30. Wada T, Penninger JM. Mitogen-activated protein kinases in apoptosis regulation. Oncogene. 2004; 23:2838–2849. [PubMed: 15077147]

31. Roskoski R. ERK1/2 MAP kinases: structure, function, and regulation. Pharmacol Res. 2012; 66:105–143. [PubMed: 22569528]

32. Ito M, Haito S, Furumoto M, Uehata Y, Sakurai A, Segawa H, Tatsumi S, Kuwahata M, Miyamoto K. Unique uptake and efflux systems of inorganic phosphate in osteoclast-like cells. Am J Physiol Cell Physiol. 2007; 292:C526–C534. [PubMed: 16971494]

33. Reynolds JL, Joannides AJ, Skepper JN, McNair R, Schurgers LJ, Proudfoot D, Jahnen-Dechent W, Weissberg PL, Shanahan CM. Human vascular smooth muscle cells undergo vesicle-mediated calcification in response to changes in extracellular calcium and phosphate concentrations: a potential mechanism for accelerated vascular calcification in ESRD. J Am Soc Nephrol. 2004; 15:2857–2867. [PubMed: 15504939]

34. Kapustin AN, Davies JD, Reynolds JL, McNair R, Jones GT, Sidibe A, Schurgers LJ, Skepper JN, Proudfoot D, Mayr M, Shanahan CM. Calcium regulates key components of vascular smooth muscle cell-derived matrix vesicles to enhance mineralization. Circ Res. 2011; 109:e1–e12. [PubMed: 21566214]

Highlights

- PiT-1 is required for ERK1/2 phosphorylation in response to elevated phosphate.
- Phosphate uptake through PiT-1 is not required for ERK1/2 phosphorylation.
- Transport-independent PiT-1 function promotes osteochondrogenic phenotype change.
- Transport-dependent and -independent PiT-1 functions are required for mineralization.

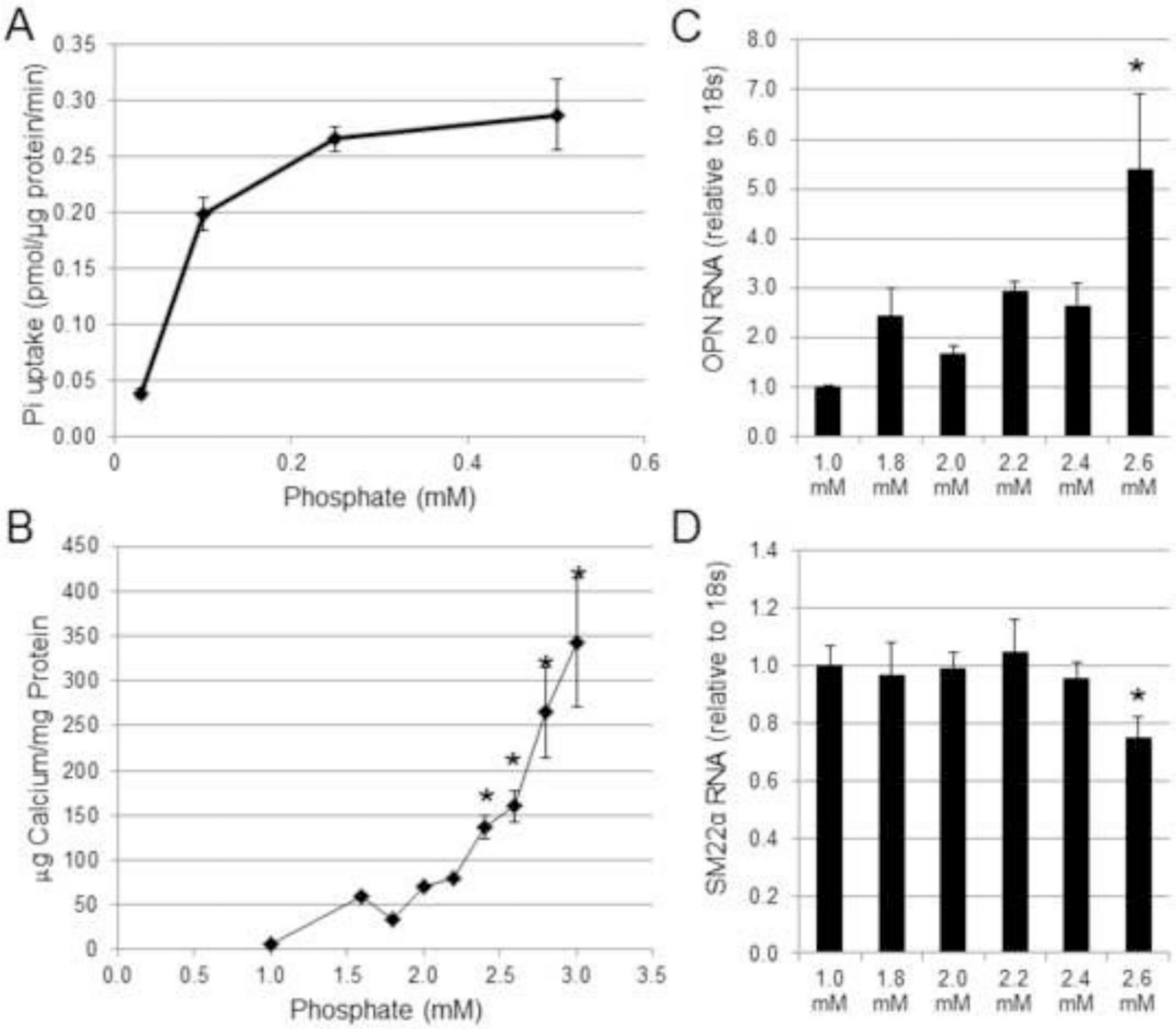

Figure 1. Concentrations of Pi above levels that support maximal Pi uptake rate are required to induce matrix mineralization and osteochondrogenic differentiation in VSMC

(A) Sodium-dependent Pi uptake was measured at different Pi concentrations (0.03 mM to 0.5 mM Pi) in VSMCs isolated from wild-type C57BL/6 mice (WT VSMCs). (B) Calcium deposition of WT VSMCs was quantified after 8 days of incubated in various Pi concentrations. (C–D) Separately, RNA lysate of WT VSMCs was collected after 6 days of Pi induction, and then (C) OPN and (D) SM22α were quantified by Q-PCR. Data are presented as mean ± standard deviation (S.D.), n = 3 for all data points. Statistically significant differences from 1.0 mM Pi data (B–D) are indicated by * = $P<0.05$ as measured by One-way ANOVA post-hoc Tukey analysis.

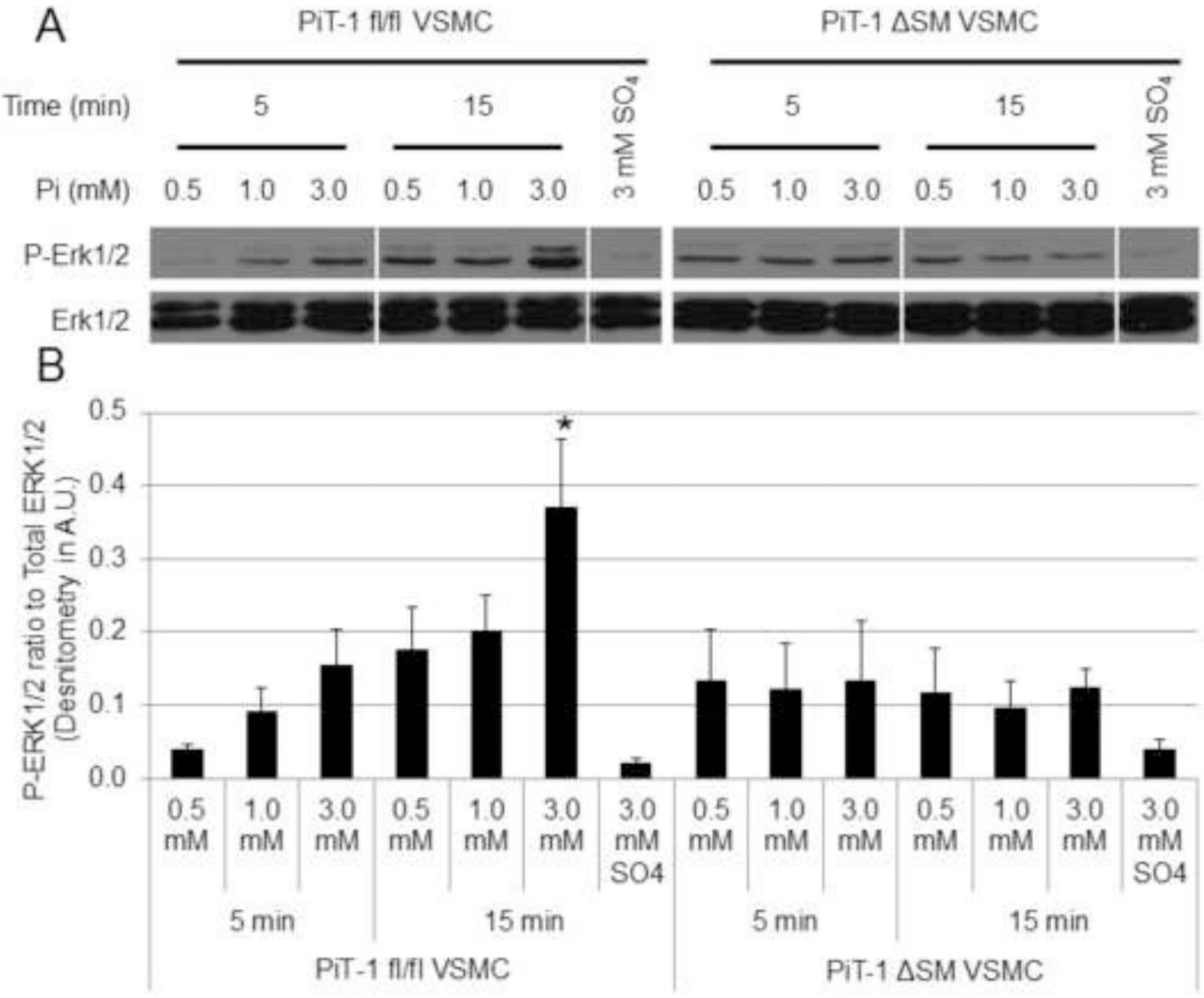

Figure 2. PiT-1 is required for Pi-induced ERK1/2 phosphorylation in VSMCs

(A) Pi induction of p-ERK1/2 and total ERK1/2 were visualized by Western blot analysis by incubating PiT-1 fl/fl and PiT-1 ΔSM VSMCs in 0.5 mM Pi, 1.0 mM Pi, 3.0 mM Pi, or 3.0 mM Sodium sulfate for 5 or 15 minutes. (B) Densitometry was used to quantify the immunoblot images and shown as the ratio of P-ERK1/2 to Total ERK1/2. Western blot is representative of three experiments with similar results, and quantification is represented as mean ± S.D., n = 3 for all data points. Statistically significant differences from all other data from the same cell line is indicated by * = $P<0.05$ as measured by One-way ANOVA post-hoc Tukey analysis.

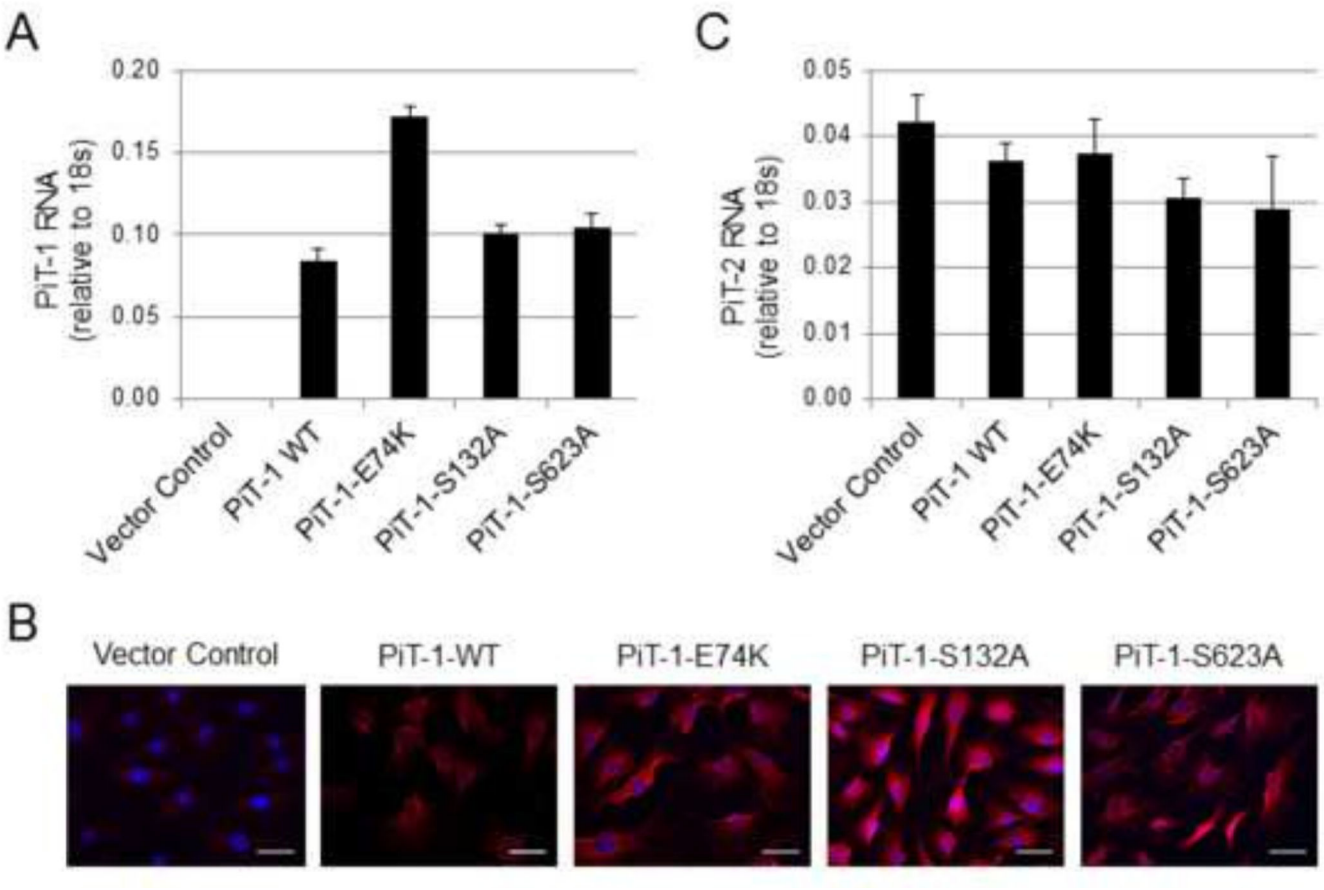

Figure 3. PiT-1 constructs transduced into PiT-1 ΔSM VSMCs are expressed and did not alter PiT-2 mRNA levels

(A) Q-PCR quantification of PiT-1 mRNA expression of PiT-1 ΔSM VSMCs transduced with vector control, PiT-1 WT, PiT-1-E74K, PiT-1-S132A, or PiT-1-S623A confirmed stable expression. (B) Immunocytochemical analysis of PiT-1 ΔSM VSMCs expressing Vector Control, PiT-1-WT, PiT-1-E74K, PiT-1-S132A, or PiT-1-S623A with primary PiT-1 antibody (red) and DAPI counterstain (blue) show expression of the PiT-1 WT, PiT-1-E74K, PiT-1-S132A, and PiT-1-S623A proteins, scale bar is 25 μm. (C) PiT-2 mRNA quantification by Q-PCR confirmed no significant effects on PiT-2 mRNA expression in any cell line. Data presented as mean ± S.D. (A,C) or representative images (B).

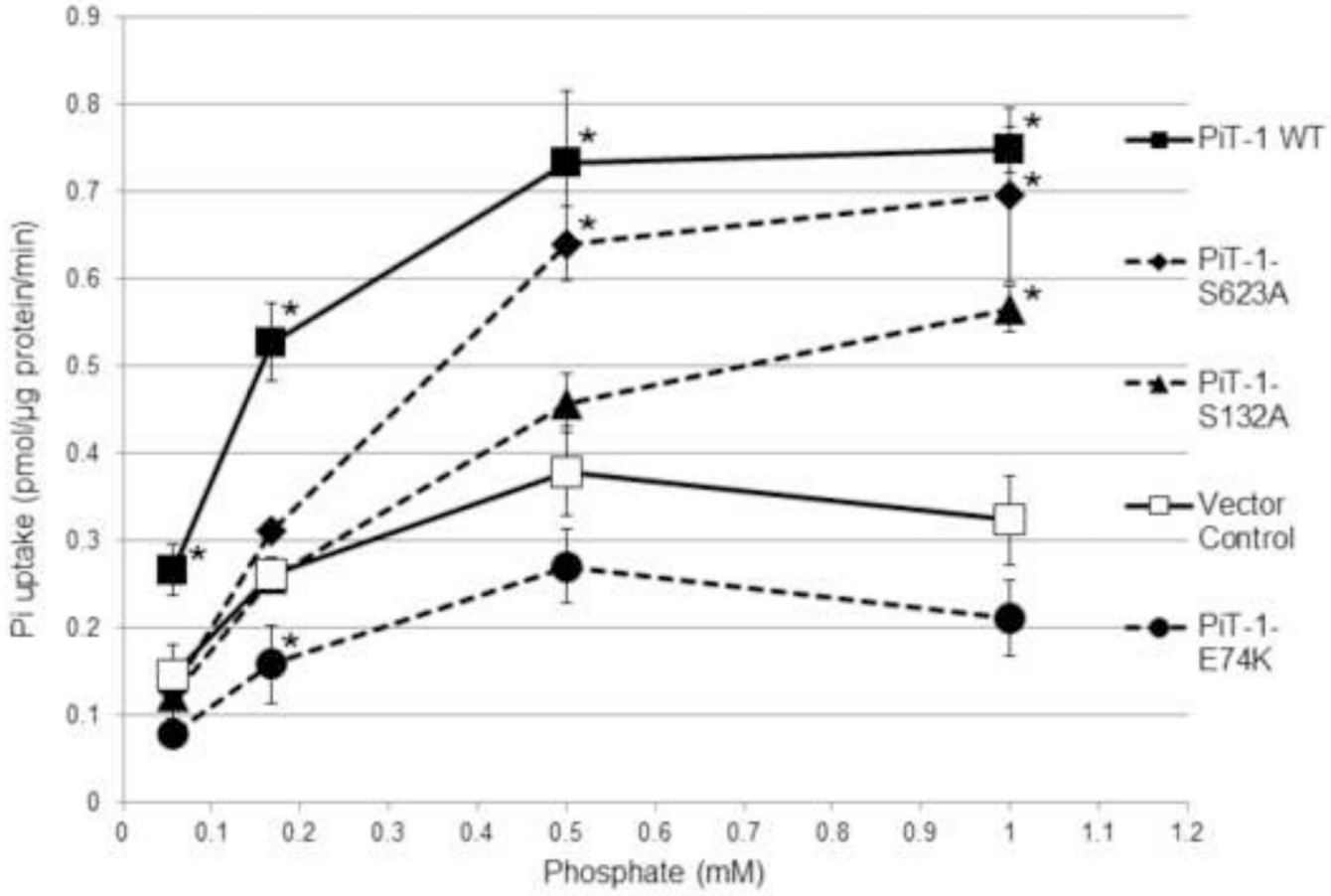

Figure 4. PiT-1 point mutations impair sodium-dependent Pi uptake in VSMCs

Sodium-dependent Pi uptake was quantified over a range of Pi concentrations in VSMCs expressing vector control, PiT-1 WT, PiT-1-E74K, PiT-1-S132A, or PiT-1-S623A. VSMC Pi uptake was measured over 20 minutes and normalized to time and VSMC protein content. Dashed connecting lines signify PiT-1 point mutation constructs. Data presented as mean ± S.D., n = 3 for all data points. Statistically significant differences between Vector Control and each PiT-1 construct at the same Pi concentration are indicated by * = $P<0.05$ as measured by One-way ANOVA post-hoc Tukey analysis.

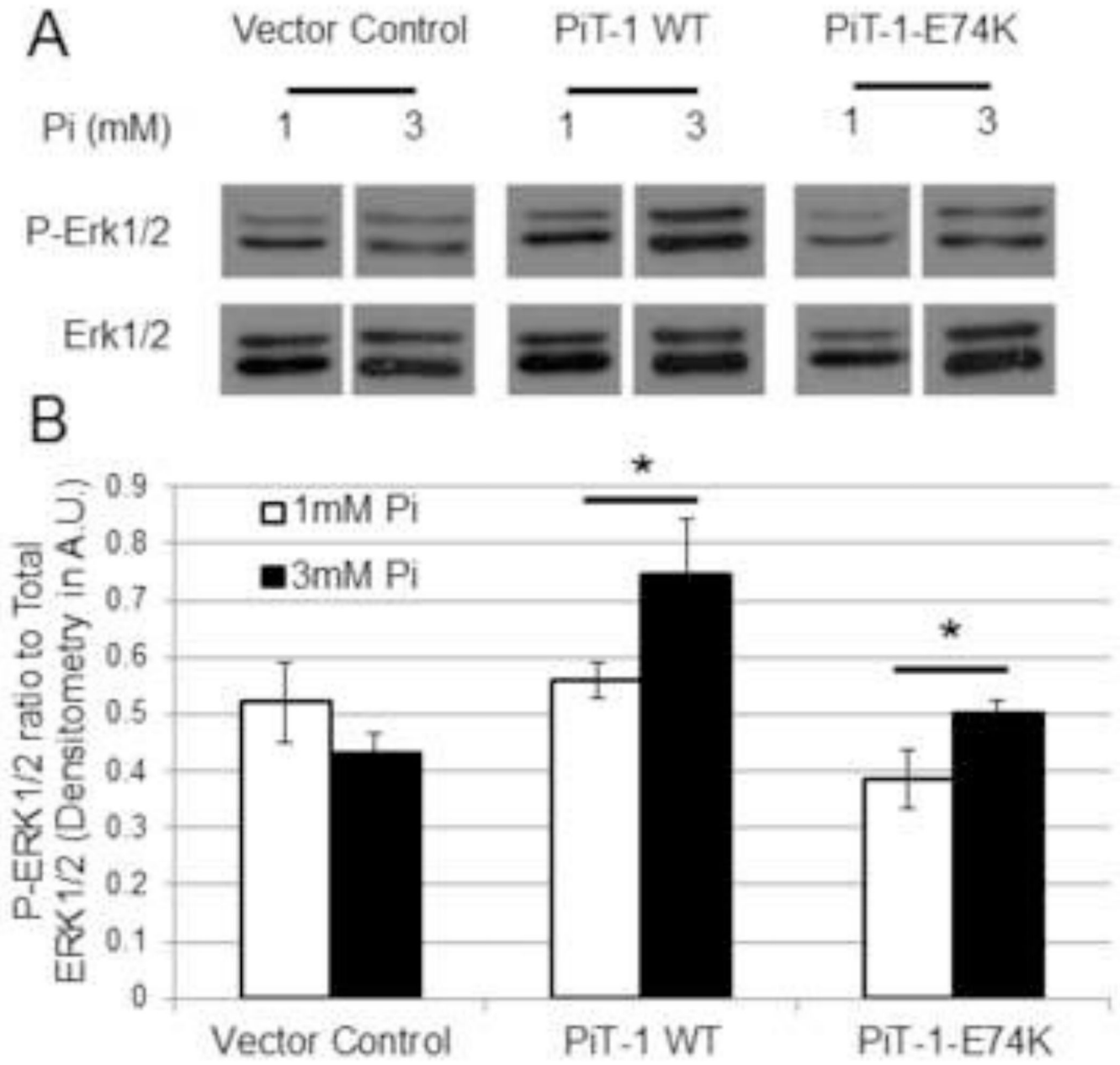

Figure 5. Elevated Pi induced ERK1/2 phosphorylation through Pi transport-independent PiT-1 function

(A) ERK1/2 phosphorylation was induced in PiT-1 ΔSM VSMCs expressing vector control, PiT-1 WT, or PiT-1-E74K with incubation in 1.0 mM or 3.0 mM Pi for 15 minutes. P-ERK1/2 and total ERK1/2 were visualized by western blot analysis. (B) Densitometry quantification of three independent experiments shows the ratio of P-ERK1/2 to Total ERK1/2. Data presented as a representative image (A) or mean ± S.D., n = 3 for all data points (B). Statistically significant differences between two independent means are indicated by * = $P<0.05$ as measured by student t-test.

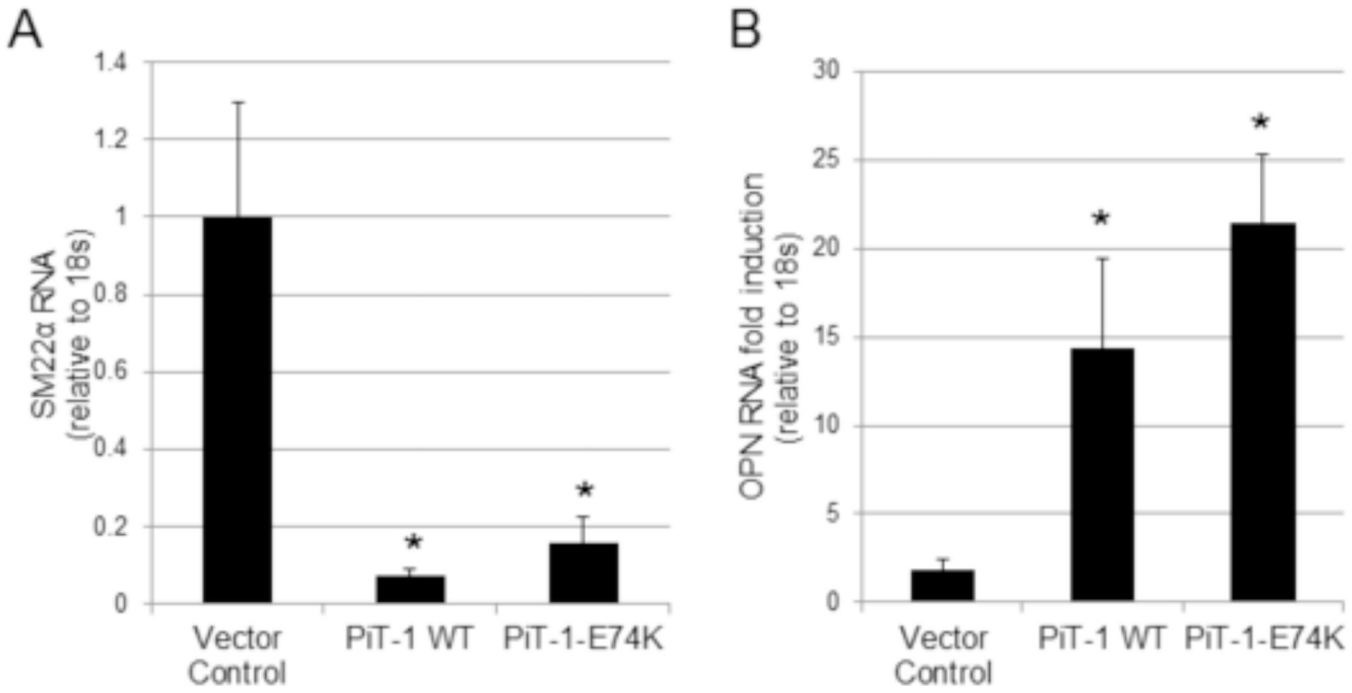

Figure 6. PiT-1 promotion of VSMC osteochondrogenic differentiation does not require Pi uptake

(A) SM22α RNA expression in PiT-1 ΔSM VSMCs expressing vector control, PiT-1 WT, or PiT-1-E74K was quantified by Q-PCR after incubation in 1.0 mM Pi for 4 days. (B) OPN RNA expression is presented as fold-induction of 2.6 mM Pi over 1.0 mM Pi after 4 days of incubation. Data presented as mean ± S.D., n = 3 for all data points. Statistically significant differences of means compared to vector control are indicated by * = $P<0.05$ as measured by One-way ANOVA post-hoc Tukey analysis.

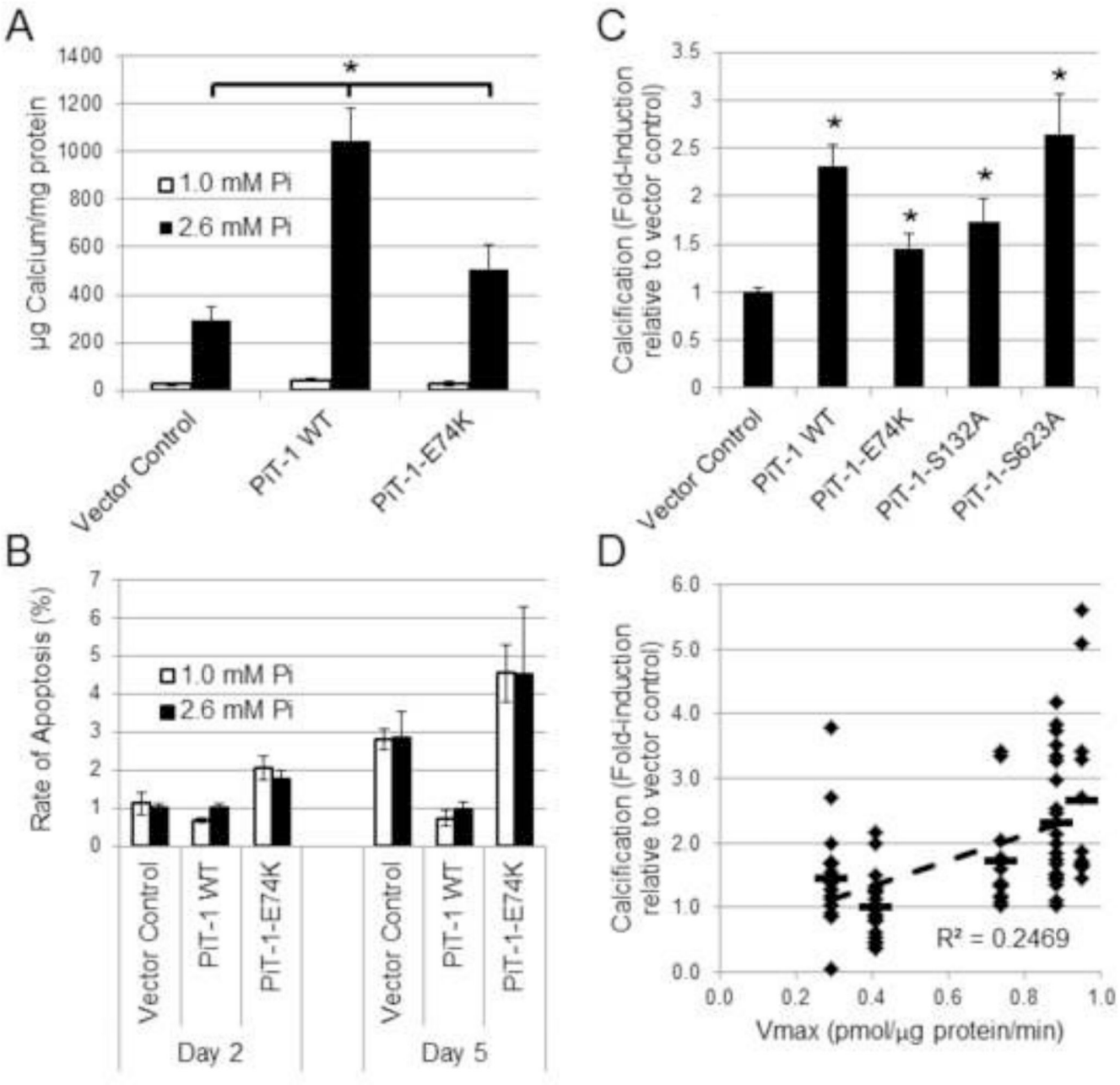

Figure 7. PiT-1 promotes VSMC matrix mineralization through both Pi uptake-dependent and -independent functions

(A) Matrix calcium content was quantified from PiT-1 ΔSM VSMCs expressing vector control, PiT-1 WT, or PiT-1-E74K that were induced to mineralize in normal Pi (1.0 mM) or elevated Pi (2.6 mM) for 8 days. (B) Rate of apoptosis was determined after incubation in normal or elevated Pi for 2 or 5 days. (C) Calcification was quantified of PiT-1 ΔSM VSMCs expressing vector control, PiT-1 WT, PiT-1-E74K, PiT-1-S132A, or PiT-1-S623A, and data is presented as fold-induction over vector control for each experiment by cell line. (D) Correlation analysis between calcification and calculated sodium-dependent Pi uptake Vmax parameter for each cell line is presented, with a horizontal dash indicating average

value of data points and a dashed regression line with the coefficient of correlation indicating linear correlation. Data is presented as mean ± S.D. (A–C), or as single points for linear regression (D). Statistically significant differences between indicated means (A) or compared to vector control (C) are indicated by * = $P<0.05$, determined by One-way ANOVA post-hoc Tukey analysis.

Table 1

Site-directed mutagenesis primers and real-time Q-PCR primers and probes.

Function	Gene	Primer Sequence (5' to 3')	Accession Number
Site-directed mutagenesis	PiT-1-E74K	F: CTTAGCTAGCATCTTCAAAACTGTGGGCTCCGC	N/A
		R: GCGGAGCCCACAGTTTTGAAGATGCTAGCTAAG	
	PiT-1-S132A	F: GCTTCGTTTTTGAAGCTTCCGATTGCTGGGACCCATTG	
		R: CAATGGGTCCCAGCAATCGGAAGCTTCAAAAACGAAGC	
	PiT-1-S623A	F: ACATTGGCCTTCCCATCGCCACAACACATTGCAAA	
		R: TTTGCAATGTGTTGTGGCGATGGGAAGGCCAATGT	
Q-PCR	OPN	F: TGAGGTCAAAGTCTAGGAGTTTCC	NM_009263
		R: TTAGACTCACCGCTCTTCATGTG	
		P: ***FAM***–TTCTGATGAACAGTATCCTG–***MGB***	
	SM22α	F: GACTGACATGTTCCAGACTGTTGAC	NM_011526
		R: CAAACTGCCCAAAGCCATTAG	
		P: ***FAM***–TGAAGGTAAGGATATGGCAGC–***MGB***	
	PiT-1	F:TTCCTTGTTCGTGCGTTCATC	NM_015747
		R:AATTGGTAAAGCTCGTAAGCCATT	
		P:***FAM***-CCGTAAGGCAGATCC-***MGB***	
	PiT-2	F:GACCGTGGAAACGCTAATGG	NM_011394
		R: CTCAGGAAGGACGCGATCAA	
		P:***FAM***-CATGGTTGGTTCAGCTG-***MGB***	

Primers and probes used in either site-directed mutagenesis or Q-PCR are listed here with the experimental function, the gene name, and the amplicon size and accession number if applicable. Primers used in site-directed mutagenesis have the desired mutation underlined. Q-PCR probes are FAM-reporters with MGB quenchers. F = Forward primer; R = Reverse primer; P = Probe.

Table 2

Essential PiT-1 amino acids and mutations that affect Pi transport.

Human PiT-1	Mouse PiT-1	Mutation
Glu70 (E70)	Glu74 (E74)	Glutamic acid → Lysine (E74K) [21]
Ser128 (S128)	Ser132 (S132)	Serine → Alanine (S132A) [22]
Ser621 (S621)	Ser623 (S623)	Serine → Alanine (S623A) [23]

Mutations in human PiT-1 that were described in previous studies to be essential for Pi transport are listed with the corresponding amino acid in mouse PiT-1. The mutation described that inhibited Pi transport is listed with the annotation describing the mouse PiT-1 mutation.